*Research Paper*
*Computational Methods for Differential Equations*
http://cmde.tabrizu.ac.ir
Vol. *, No. *, *, pp. 1-17
DOI:10.22034/cmde.2026.67058.3179

# A robust semi-analytical technique for solving third-order non-linear Emden-Fowler equations

**Mithilaba M. Chudasama**[1], **Yogeshwari F. Patel**[1], **and Mohammad Izadi**[2,*]

[1]Department of Mathematical Sciences, P D Patel Institute of Applied Sciences, Charotar University of Science & Technology, Changa, Gujarat-388421, India.

[2]Department of Applied Mathematics, Faculty of Mathematics and Computer, Shahid Bahonar University of Kerman, Kerman, Iran.

**Abstract**

This study presents a robust semi-analytical algorithm for solving third-order nonlinear Emden–Fowler type equations, which frequently arise in astrophysics, chemical reactor theory, and mathematical physics. The proposed algorithm leverages the Differential Transform Method (DTM) to simplify the complexities introduced by nonlinear terms, transforming them into manageable algebraic equations. The novelty of this approach lies in its ability to handle singular behavior at $x = 0$ while maintaining high computational efficiency and accuracy. Rigorous error analysis confirms the algorithm's rapid convergence and superior accuracy compared to existing methods. Numerical experiments validate the theoretical predictions, highlighting the algorithm's effectiveness and reliability in solving complex nonlinear differential equations.

**Keywords.** Non-linear Emden-Fowler equation, Differential transform method, Error analysis, Convergence analysis.
**2010 Mathematics Subject Classification.** 65L20; 34A25; 34A34.



## 1. Introduction

In theoretical and mathematical physics, nonlinear singular boundary value problems are frequently used to model various real-world phenomena derived from scientific material science. Jonathan Homer Lane, a theoretical physicist, first introduced the nonlinear singular boundary value problem in 1846 to study the heating efficiency of a spherical gas cloud under classical thermodynamics [22]. Over the years, these equations have been instrumental in modeling numerous scientific phenomena, including stellar structure [8], isothermal gas spheres [9], catalytic diffusion reactions [16, 23], heat conduction associated with the human head [11, 18], and electrohydrodynamic flow problem [14, 24] to name a few. We consider the higher-order nonlinear Emden-Fowler type singular differential equation (EFSDE) in its general form [39, 40]:

$$x^{-\lambda}\frac{d^n}{dx^n}\left(x^{\lambda}\frac{d^m}{dx^m}\right)s + \chi(x)h(x,s) = 0, \tag{1.1}$$

where $\chi(x)$ and $h(x,s)$ are familiar continuous real-valued functions, and $\lambda$ signifies the shape factor. Equation (1.1) encompasses various nonlinear singular problems depending on the values of $n$, $m$, and $h(x,s)$:

(i) When $n = m = 1$, Eq. (1.1) simplifies to the second-order Lane-Emden-Fowler equation:

$$x^{-\lambda}\frac{d}{dx}\left(x^{\lambda}\frac{d}{dx}\right)s + \chi(x)h(x,s) = 0. \tag{1.2}$$

This equation arises, for instance, in heat explosion analysis [9], quantum mechanics [32], and non-isothermal reaction-diffusion systems [30].

Received: 29 April 2025; Accepted: 25 May 2026.
∗ Corresponding author. Email: izadi@uk.ac.ir; mohamad.izadi@gmail.com.

(ii) Setting $\chi(x) = 1$ and $h(s) = s^m$ yields the classical Lane-Emden equation, which models polytropic stellar interiors [29].
(iii) For $\chi(x) = 1$ and $h(s) = e^s$, Eq. (1.1) becomes the second-type Lane-Emden equation, describing isothermal gas spheres.

Third-order EFSDEs are derived by setting $m + n = 3$ with $m, n \geq 1$ in Eq. (1.1), leading to two cases:
**Case I:** Let $m = 1$ and $n = 2$, resulting in:

$$s'''(x) + \frac{2\lambda}{x}s''(x) + \frac{\lambda(\lambda-1)}{x^2}s'(x) + \chi(x)g(s) = 0. \tag{1.3}$$

Here, $x = 0$ exhibits multisingularity with shape factors $2\lambda$ and $\lambda(\lambda - 1)$.
**Case II:** Let $m = 2$ and $n = 1$, yielding:

$$s'''(x) + \frac{\lambda}{x}s''(x) + \chi(x)g(s) = 0. \tag{1.4}$$

A singularity occurs at $x = 0$ in this scenario, characterized by the shape factor $\lambda$. For Eqs. (1.3) and (1.4), the boundary conditions over the domain $\Omega = [x_0, x_1]$ include:

**Type I:** $s(x_0) = s_0$, $s'(x_0) = s_1$, $s''(x_0) = s_2$,
**Type II:** $s(x_0) = s_0$, $s'(x_0) = s_1$, $s(x_1) = s_2$,
**Type III:** $s(x_0) = s_0$, $s'(x_0) = s_1$, $s'(x_1) = s_2$.

Here, the parameters $s_i$ for $i = 0, 1, 2$ are given real numbers. The dual challenges of a singular point at $x = 0$ and the highly nonlinear structure of $h(x, s)$ make analytical approaches exceptionally demanding. Some semi-analytical approaches developed to address Eqs. (1.3)–(1.4) include the variational iteration methodology (VIM) [39], the Adomian decomposition method (ADM) [40], the differential transform method (DTM) [7], and the optimal homotopy analysis technique [35]. These methods leverage series expansions, recurrence relations, or iterative schemes to handle nonlinear terms and singularities, though their accuracy often depends on truncation limits or convergence criteria. Consequently, developing high-order, computationally efficient numerical algorithms remains crucial for robust solutions. Recent advances in numerical strategies encompass the cubic B-spline collocation scheme [13], the Bernoulli polynomial-based collocation method [34], uniform Haar wavelet discretization [37], artificial neural networks with adaptive learning [33, 38], Bernoulli and Hermite wavelet techniques [20], the spectral Legendre, Jacobi, and Chebyshev approaches [3, 10, 41], the Vieta-Fibonacci-quasilinearization methodology [15], and the combined quasilinearization and quintic trigonometric B-spline collocation scheme [6]. Other methods proposed to solve various orders of singular Lane-Emden-Fowler equations can be found in Refs. [1, 4, 5, 17, 19, 21, 31]. Each method offers distinct trade-offs between computational complexity, convergence rate, and implementation ease, highlighting the need for context-specific algorithm selection.

In this work and by extending the above-mentioned research studies, we propose a robust semi-analytical algorithm, the DTM to address third-order EFSDEs (1.3)–(1.4). The DTM, rooted in Taylor series expansions, transforms differential equations into algebraic recurrence relations, enabling efficient handling of nonlinearities and singularities without spatial discretization [25–28, 36]. Key contributions include:

- Analytical approximation capability through recursive algebraic systems,
- Effective handling of singular terms via term-wise transformation, avoiding L'Hospital's rule,
- Reduced computational cost by bypassing numerical quadrature or collocation matrices,
- Adaptability to both initial and boundary value problems with high accuracy.

The proposed algorithm outperforms existing methods such as ADM [12], VIM [39], and the new cubic B-spline scheme (NCBS) [13] in simplicity and analytical tractability. Numerical experiments validate its convergence and accuracy. The subsequent sections of this research work are arranged as: Section 2 details the fundamentals of DTM, discusses its convergence and error analysis, and illustrates the application of DTM to a special case (ii) of the model problem (1.1). Section 3 presents four numerical test examples that demonstrate the practical implementation and efficacy of the suggested algorithm. Finally, Section 4 concludes the study and outlines potential future work.

## 2. DTM: The Proposed Semi-analytical Technique

Here, we introduce a method generating rapidly convergent successive approximations, showing equal effectiveness for linear and nonlinear cases. This powerful method offers two key advantages: (1) high efficiency in obtaining solutions, and (2) versatility in handling both exact and approximate formulations. Its applications span technology, finance, engineering, and natural science disciplines (physics, chemistry, biology, and earth science). This section presents a basic definition and the essential properties of a differential transform for the reader's better understanding.

**Definition 2.1.** *In the time domain $\Im$, a differential transformation of an analytic function $y(x)$ is given by*

$$\zeta(\kappa) = \frac{1}{\kappa!}\left[\frac{d^{\kappa} y(x)}{dx^{\kappa}}\right]_{x=0}. \tag{2.1}$$

**Definition 2.2.** *Inverse differential transformation of $\zeta(\kappa)$ is given by*

$$y(x) = \sum_{\kappa=0}^{\infty} \zeta(\kappa)\, x^{\kappa}. \tag{2.2}$$

Using Eqs. (2.1) and (2.2), we get

$$y(x) = \sum_{\kappa=0}^{\infty} \frac{1}{\kappa!}\left[\frac{d^{\kappa} y(x)}{dx^{\kappa}}\right]_{x=0} x^{\kappa}. \tag{2.3}$$

The following Table 1 outlines fundamental operations of the DTM where $y(x)$ is original functions and $Y(k)$ is differential transforms of original function.

### 2.1. Analysis of convergence behavior and error estimation.

The error analysis examines the discrepancies between the series solutions and exact results, typically quantifying truncation and rounding errors to assess accuracy. In the following, we will state and prove a theorem related to the convergence analysis of our method.

**Theorem 2.3.** *Consider an operator $\Omega : H \to H$ on a Hilbert space $H$, and let $g(\eta)$ denote the exact solution of Eq. (1.4). The series $\sum_{i=0}^{\infty} \zeta_i$, derived from the expansion $\sum_{k=0}^{\infty} \zeta_k\, x^k$, converges to $g(\eta)$ if there exists a constant $\gamma \in [0, 1)$ such that*

$$\|\zeta_{k+1}\| \le \gamma \|\zeta_k\| \quad \forall k \in \mathbb{N}_0 := \mathbb{N} \cup \{0\}.$$

*For further details, see [28].*

*Proof.* We express the partial sum in the form

$$\begin{aligned}
&S_0 = 0,\\
&S_1 = S_0 + \zeta_1 = \zeta_1,\\
&S_2 = S_1 + \zeta_2 = \zeta_1 + \zeta_2,\\
&\quad\vdots\\
&S_N = S_{N-1} + \zeta_N = \zeta_1 + \zeta_2 + \zeta_3 + \cdots + \zeta_N.
\end{aligned}$$

We shall now demonstrate that the sequence $\{S_N\}_{N=0}^{\infty}$ forms a Cauchy sequence in the Hilbert space $H$. We have

$$\|S_{N+1} - S_N\| = \|\zeta_{N+1}\| \le \gamma \|\zeta_N\| \le \gamma^2 \|\zeta_{N-1}\| \le \ldots \le \gamma^{N+1} \|\zeta_0\|.$$

Take $N, M \in \mathbb{N}, N \ge M$, we get

$$\begin{aligned}
\|S_N - S_M\| &= \big\|(S_N - S_{N-1}) + (S_{N-1} - S_{N-2}) + \cdots + (S_{M+2} - S_{M+1}) + (S_{M+1} - S_M)\big\|\\
&\le \|S_N - S_{N-1}\| + \|S_{N-1} - S_{N-2}\| + \cdots + \|S_{M+2} - S_{M+1}\| + \|S_{M+1} - S_M\|\\
&\le \gamma^{N+1}\|\zeta_0\| + \gamma^{N+2}\|\zeta_0\| + \gamma^{N+3}\|\zeta_0\| + \ldots\\
&\le \big(\gamma^{N+1} + \gamma^{N+2} + \gamma^{N+3} + \ldots\big)\|\zeta_0\|
\end{aligned}$$

TABLE 1. The operational foundation of DTM [36].

| Function | Differential Transform |
|---|---|
| $y(t) = \alpha\, f(t) \pm \beta\, g(t)$ | $Y(\kappa) = \alpha\, F(\kappa) \pm \beta\, G(\kappa)$, ($\alpha$, $\beta$ are constants) |
| $y(t) = \frac{d^m g(t)}{dt^m}$ | $Y(\kappa) = (\kappa+1)(\kappa+2)\dots(\kappa+m)G(\kappa+m)$ |
| $y(t) = f(t)g(t)$ | $Y(k) = \sum_{l=0}^{\kappa} F(l)G(\kappa-l)$ |
| $y(t) = t^m$ | $\delta(\kappa-m) = \begin{cases} 1, & \kappa = m \\ 0, & \kappa \neq m \end{cases}$ |
| $y(t) = e^{at}$ | $Y(\kappa) = \frac{a^\kappa}{\kappa!}$ |
| $y(t) = (1+t)^m$ | $Y(\kappa) = \frac{m(m-1)(m-2)\dots(m-\kappa+1)}{k!}$ |
| $y(t) = \sin(\omega t + \alpha)$ | $Y(\kappa) = \frac{\omega^\kappa}{\kappa!} \sin\left(\frac{\pi\kappa}{2} + \alpha\right)$ |
| $y(t) = \cos(\omega t + \alpha)$ | $Y(\kappa) = \frac{\omega^k}{k!} \cos\left(\frac{\pi\kappa}{2} + \alpha\right)$ |
| $y(t) = g_1(t)\, g_2(t) \dots g_n(t)$ | $Y(k) = \sum_{\kappa_1=0}^{\kappa} \sum_{\kappa_2=0}^{\kappa_1} \dots \sum_{\kappa_{n-1}=0}^{\kappa_{n-2}} G_1(\kappa_1)\, G_2(\kappa_2-\kappa_1) \dots G_n(\kappa_{n-1})$ |
| $f(y) = y^m$ | $F(\kappa) = \begin{cases} Y^m(0), & \kappa = 0, \\ \frac{1}{Y(0)} \sum_{l=1}^{\kappa} \frac{(m+1)l-\kappa}{\kappa} Y(l)F(\kappa-l), & \kappa \geq 1. \end{cases}$ |
| $f(y) = e^{qy}$ | $F(\kappa) = \begin{cases} e^{qY(0)}, & \kappa = 0, \\ q \sum_{l=0}^{\kappa-1} \frac{l+1}{\kappa} Y(l+1)F(\kappa-l-1), & \kappa \geq 1. \end{cases}$ |

$$= \frac{\gamma^{N+1}}{1-\gamma}\|\zeta_0\|,$$

This established that $\lim_{N,M\to\infty} \|S_N - S_M\| = 0$ proving $\{S_n\}_{n=0}^{\infty}$ is a Cauchy sequence in the Hilbert space $H$. By completeness, there exists $S \in H$ such that $S_N \to S$. Here, $\|\cdot\|$ denotes the infinity norm (i.e., the supremum norm). □

**Remark 2.4.** *For every $i \in \mathbb{N}_0$, the numbers $\gamma_i$ in Theorem 2.3 can be defined as*

$$\gamma_i = \begin{cases} \frac{\|\zeta_{i+1}\|}{\|\zeta_i\|}, & \text{if } \|\zeta_i\| \neq 0, \\ 0, & \text{if } \|\zeta_i\| = 0. \end{cases}$$

**Corollary 2.5.** *If $0 \leq \gamma_i < 1$ for $i = 1, 2, 3, \dots$, then the series form $\sum_{i=0}^{\infty} \zeta_i$ converges to the exact solution.*

2.1.1. *Residual Error and Maximum Residual Error.* To evaluate the accuracy and effectiveness of the DTM solution for the model (1.1), the residual and the maximum absolute residual errors are defined as used in [42],

$$\mathrm{Res}_i(x) = \left| x^{-\lambda} \frac{d^n}{dx^n} \left( x^\lambda \frac{d^m}{dx^m} \right) S_i + \chi(x)\, h(x, S_i) \right|, \tag{2.4}$$

$$\mathrm{R}_i = \max_{0 \leq x \leq 1} \mathrm{Res}_i(x), \quad 1 \leq i \leq N, \tag{2.5}$$

for fixed values of $m, n$. Here, each $S_i$ represents the $i$-th partial sum of the series solution generated by the DTM.

## 3. Numerical Results

To validate the performance of DTM, three benchmark test examples spanning linear and nonlinear differential equations with various initial and boundary conditions will be solved with known analytical solutions. The computational outcomes obtained via DTM are rigorously compared with those from established available techniques such as the variational iteration methodology (VIM) [39], new cubic B-spline scheme (NCBS) [13], and Adomian decomposition method (ADM) [12]. Quantitative metrics, including absolute error norms, convergence rates, and computational efficiency, were analyzed to assess accuracy and robustness. Additionally, we utilize the Python software package to derive the coefficients in DTM.

**Test problem 3.1.** *Consider parameter values as $m = 2, n = 1, \lambda = 2$, Eq. (1.1) reduces to the second kind of third-order nonlinear EFSDE [2]:*

$$\frac{d^3s}{dx^3} + \frac{2}{x}\frac{d^2s}{dx^2} - \frac{25}{8}\left(16x^2 + 52x^5 + 7x^{10}\right)s^7 = 0. \tag{3.1}$$

*Considering $x_0 = 0, x_1 = 1, s_0 = s_1 = s_2 = 0$, one gets Type II boundary conditions given as:*

$$s(0) = 1,\ s'(0) = 0,\ s''(0) = 0. \tag{3.2}$$

*The true analytical form of solution related to Test problem (3.1) is $\frac{1}{\sqrt{1-x^5}}$.*

Applying fundamental properties of DTM to Eqs. (3.1) and (3.2), we have

$$8\sum_{l=0}^{k}\delta(l-1)(k+3-l)(k+2-l)(k+1-l)S(k+3-l) + 16(k+1)(k+2)S(k+2)$$
$$-25\sum_{l=0}^{k}\Big(16\delta(l-3) + 52\delta(l-8) + 7\delta(l-13)\Big)E(k-l) = 0. \tag{3.3}$$

Here, we have

$$E(k) = \begin{cases} S^7(0), & k = 0, \\ \frac{1}{S(0)}\sum\limits_{l=1}^{k}\frac{8l-k}{k}S(l)E(k-l), & k \geq 1, \end{cases} \tag{3.4}$$

and the transformed initial conditions are

$$S(0) = 1, \quad S(1) = 0, \quad S(2) = 0. \tag{3.5}$$

Through the application of DTM, we derive a series-based analytical solution, with coefficients determined computationally via Python. The coefficients are initialized by evaluating $S(0)$, $S(1)$, and $S(2)$ from the initial conditions stated in Eq. (3.4). Subsequently, $S(3)$ and $S(4)$ are found by inserting $k = 1$ and $k = 2$ into Eq. (3.3). In order to facilitate the reader's understanding, we include a few reference evaluations. For $k = 1$, Eq. (3.3) reduces to

$$8\sum_{l=0}^{1}\delta(l-1)(4-l)(3-l)(2-l)S(4-l) + 16(2)(3)S(3) - 25\sum_{l=0}^{1}\Big(16\delta(l-3) + 52\delta(l-8)$$
$$+ 7\delta(l-13)\Big)E(1-l) = 0. \tag{3.6}$$

Using Eq. (3.4) and the transformed initial condition in Eq. (3.5), Eq. (3.6) gives $S(3) = 0$. For $k = 2$, Eq. (3.3) reduces to

$$8\sum_{l=0}^{2}\delta(l-1)(5-l)(4-l)(3-l)S(5-l) - 25\sum_{l=0}^{2}\Big(16\delta(l-3) + 52\delta(l-8) \tag{3.7}$$
$$+ 7\delta(l-13)\Big)E(2-l) + 192S(4) = 0.$$

Using Eq. (3.4), the transformed initial condition in Eq. (3.5), and $S(3) = 0$, Eq. (3.7) reduces to $S(4) = 0$. For $k = 2$, Eq. (3.3) simplifies to

$$8\sum_{l=0}^{3}\delta(l-1)(6-l)(5-l)(4-l)S(6-l) - 25\sum_{l=0}^{3}\Big(16\delta(l-3)+52\delta(l-8)+7\delta(l-13)\Big)E(3-l)+320S(5)=0. \tag{3.8}$$

Using Eq. (3.4) and the transformed initial condition in Eq. (3.5), $S(3) = 0$ and $S(4) = 0$, Eq. (3.7) reduces to $S(5) = \frac{1}{2}$. By repeatedly substituting values of $k$ into Eq. (3.3) and utilizing the coefficients $S(0), S(1), S(2), S(3), S(4), S(5)$, and the coefficients $S(k)$ for various values of $k$ are computed. Then, by applying the inverse transform formula defined in Eq. (2.2), we obtain the approximate series solution:

$$s(x) = 1 + 0.5x^5 + 0.375x^{10} + 0.3125x^{15} + 0.2734375x^{20} + \dots. \tag{3.9}$$

For analytical validation, the 15th-order DTM series solution is compared with the exact solution, $s(x) = \frac{1}{\sqrt{1-x^5}}$ as illustrated in Figure 1. The figure demonstrates excellent agreement between the two solutions. Table 2 represents a comparison of the exact solution and the DTM approximation for selected values of $x$. The absolute error highlights the accuracy and convergence of the DTM-based approach. To show the convergence of the approximate series solution obtained by DTM of Test problem 3.1 given in Eq. (3.1) and from Corollary 2.5 we have,

$$\gamma_0 = \frac{\|\zeta_1\|}{\|\zeta_0\|} < 1, \quad \gamma_1 = \frac{\|\zeta_2\|}{\|\zeta_1\|} < 1, \quad \gamma_2 = \frac{\|\zeta_3\|}{\|\zeta_2\|} < 1, \quad \dots.$$

Consequently, for the series form Eq. (3.9), $\gamma_n$ tends to 0 as $n$ tends to infinity. Therefore, from Corollary 2.5 we can say that the obtained approximate solution is convergent to the exact solution. The maximum residual error is

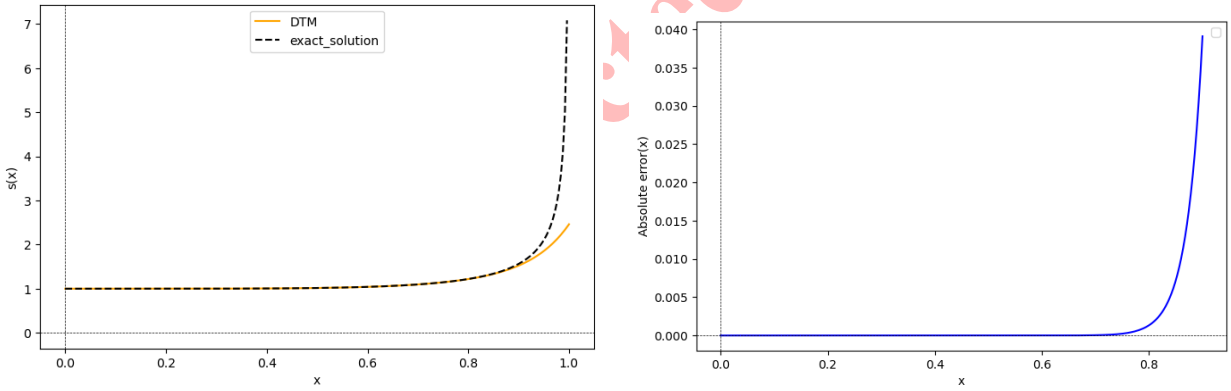


FIGURE 1. Comparison between exact solution and DTM solution of order 14 (left panel) and the related absolute error (right panel) in Test problem 3.1.

evaluated at $x = 0.5$, and the corresponding values for each order of approximation are summarized in Table 3. From the data shown in Table 3, it is observed that the maximal residual error reduces rapidly as the series order increases. At $N = 5$, the error is relatively high, but this decreases sharply to $2.560670 \times 10^{-1}$ at $N = 10$, and continues to drop to $4.596894 \times 10^{-5}$ at $N = 25$. This exponential decay in error magnitude demonstrates the efficiency and accuracy of the DTM in approximating the exact solution. These findings indicate that even for strongly nonlinear problems with singularities, DTM is capable of yielding highly accurate solutions with only moderate increases in the series order. The minimal residual error at higher orders affirms the suitability of the method for solving complex EFSDEs with precision, making it a valuable analytical tool in the study of singular boundary value problems.

TABLE 2. Comparison between the exact solution and the DTM approximation for various values of $x$ in Test problem 3.1.

| $x$ | Exact solution | DTM | Absolute error |
|---|---|---|---|
| 0.0 | 1 | 1 | 0 |
| 0.1 | 1.0000050000375003 | 1.0000050000375003 | $0.000000 \times 10^{+0}$ |
| 0.2 | 1.0001600384102430 | 1.0001600384102430 | $0.000000 \times 10^{+0}$ |
| 0.3 | 1.0012172188310886 | 1.0012172188310675 | $2.109424 \times 10^{-14}$ |
| 0.4 | 1.0051596601787673 | 1.0051596601507970 | $2.797029 \times 10^{-11}$ |
| 0.5 | 1.0160010160015240 | 1.0160010084509850 | $7.550539 \times 10^{-9}$ |
| 0.6 | 1.0413051651230136 | 1.0413044117159145 | $7.534071 \times 10^{-7}$ |
| 0.7 | 1.0963686463811178 | 1.0963296167875147 | $3.902959 \times 10^{-5}$ |
| 0.8 | 1.2195847484251134 | 1.2182529544169194 | $1.331794 \times 10^{-3}$ |
| 0.9 | 1.5626716896710573 | 1.5235840103066867 | $3.908768 \times 10^{-2}$ |

TABLE 3. Maximum residual error for Test problem 3.1.

| $N$ | 5 | 10 | 15 | 20 | 25 |
|---|---|---|---|---|---|
| $R_N$ | 2.853990 | $2.560670 \times 10^{-1}$ | $1.675247 \times 10^{-2}$ | $9.252909 \times 10^{-4}$ | $4.596894 \times 10^{-5}$ |

**Test problem 3.2.** *In the second test case, we take $m = 2$, $n = 1$, $\lambda = 2$. Then, Eq. (1.1) reduces to the second kind of third-order nonlinear EFSDE:*

$$\frac{d^3s}{dx^3} + \frac{2}{x}\frac{d^2s}{dx^2} - \frac{9}{8}\left(\frac{x^6+8}{s^5}\right) = 0. \tag{3.10}$$

*By setting $x_0 = 0, x_1 = 1, s_0 = s_1 = s_2 = 0$, we have the Type I boundary conditions given as:*

$$s(0) = 1, \quad s'(0) = 0, \quad s''(0) = 0. \tag{3.11}$$

*Although the nonlinear term contains $\frac{1}{s^5}$, the imposed initial condition $s(0) = 1$ ensures that the solution remains nonzero in a neighborhood of the origin. Therefore, the problem remains locally well-posed and the singularity at $x = 0$ is not encountered in the considered domain. One can easily check that $s(x) = \sqrt{1+x^3}$ is the exact solution of model problem 3.2.*

Rearranging Eq. (3.10) and applying fundamental properties of DTM, following recursive formula is obtained:

$$\begin{aligned} &8\sum_{l=0}^{k}\sum_{m=0}^{l}\delta(m-1)E(l-m)(k+3-l)(k+2-l)(k+1-l)S(k+3-l) \\ &+16\sum_{l=0}^{k}E(l)(k+1-l)(k+2-l)S(k+2-l) = 9(\delta(k-7)) + 72\delta(k-1), \end{aligned} \tag{3.12}$$

where

$$E(k) = \begin{cases} S^5(0), & \text{if } k = 0, \\ \frac{1}{S(0)}\sum_{l=1}^{k}\frac{6l-k}{k}S(l)E(k-l), & \text{if } k \geq 1, \end{cases} \tag{3.13}$$

and the transformed I.C. and B.C. conditions are

$$S(0) = 1, \quad S(1) = 0, \quad S(2) = 0. \tag{3.14}$$

DTM is employed to obtain an analytical series solution, and its coefficients are calculated using Python. The values of $S(0)$, $S(1)$, and $S(2)$ are derived from the initial and boundary conditions specified in Eq. (3.11). Similarly, by substituting $k = 0$ and $k = 1$ into Eq. (3.12), the coefficients $S(3)$ and $S(4)$ are computed. To compute $S(3)$, we substitute $k = 1$ into Eq. (3.12), leading to the double summation expression:

$$8\sum_{l=0}^{1}\sum_{m=0}^{l}\delta\,(m-1)\,E(l-m)\,(4-l)\,(3-l)\,(2-l)\,S\,(4-l)+16\sum_{l=0}^{1}E(l)(2-l)(3-l)S(3-l)=72. \tag{3.15}$$

By simplifying Eq. (3.15) appropriately and using transformed I.C. and B.C. (3.14), we arrive at the value $S(3) = \frac{1}{2}$. For $k = 2$, Eq. (3.12) leads to the double summation expression:

$$\begin{aligned}&8\sum_{l=0}^{2}\sum_{m=0}^{l}\delta\,(m-1)\,E(l-m)\,(5-l)\,(4-l)\,(3-l)\,S\,(5-l)+16\sum_{l=0}^{2}E(l)(3-l)(4-l)S(4-l)\\&=9(\delta(2-7))+72\delta(2-1).\end{aligned} \tag{3.16}$$

Simplification of Eq. (3.16) results in:

$$S(4)=-\frac{144S(3)E(1)-32E(2)S(2)}{384}. \tag{3.17}$$

Applying the recursive definition of $E(2)$, we get

$$E\,(2)=\frac{1}{S\,(0)}\sum_{l=1}^{2}\frac{6l-2}{2}S\,(l)\,E\,(2-l). \tag{3.18}$$

By utilizing known values $S(0)$, $S(1)$, $S(2)$, $S(3)$, we obtain $E(2) = 0$ and $S(4) = 0$. By repeatedly substituting values of $k$ into Eq. (3.3) and utilizing the coefficients $S(0), S(1)$, $S(2)$, $S(3), S(4), S(5)$, and the coefficients $S(k)$ for various values of $k$ are computed. Then, by applying the inverse transform formula defined in Eq. (2.2), we obtain the approximate series solution:

$$s(x)=1+0.5x^3-0.125x^6+0.625x^9+\ldots. \tag{3.19}$$

To assess the analytical performance of the DTM, Figure 2 compares the 9th-order series approximation with the actual solution $s(x) = \sqrt{1+x^3}$. This comparison reveals excellent agreement for small $x$, with enhanced accuracy achieved through higher-order approximations. Table 4 highlights the absolute error of the DTM solution, demonstrating its superior accuracy, particularly for smaller values of $x$. To show the convergence of the approximate series solution obtained by DTM of Test problem 3.2 given in Eq. (3.10) and from Corollary 2.5 we have,

$$\gamma_0=\frac{\|\zeta_1\|}{\|\zeta_0\|}<1,\quad \gamma_1=\frac{\|\zeta_2\|}{\|\zeta_1\|}<1,\quad \gamma_2=\frac{\|\zeta_3\|}{\|\zeta_2\|}<1,\quad \ldots.$$

Thus, for the series form in Eq. (3.19), it follows that $\gamma_n \to 0$ as $n \to \infty$. herefore, from Corollary 2.5 we can say that the obtained approximate solution is convergent to the exact solution. To assess the accuracy and convergence behaviour of the DTM for the nonlinear third-order singular differential equation described in Eq. (3.10), the residual error is computed for increasing values of the series order $N = 3, 6, 9, 12, 15$. The boundary conditions specified in Eq. (3.11) correspond to a Type I formulation. The exact analytical solution for this problem is known to be $s(x) = \sqrt{1+x^3}$ . The residual errors at various orders are summarized in Table 5. From the data, it is evident that increasing the order of approximation significantly reduces the residual error initially from $N = 3$ to $N = 5$, indicating improved accuracy. However, beyond $N = 10$, the residual error approaches a saturation point near unity. This trend suggests that while higher-order DTM solutions do converge towards the exact solution, the rate of convergence diminishes at higher orders. Nonetheless, the 15th-order solution demonstrates a high level of accuracy, confirming the robustness of the DTM for nonlinear boundary value problems of this nature.

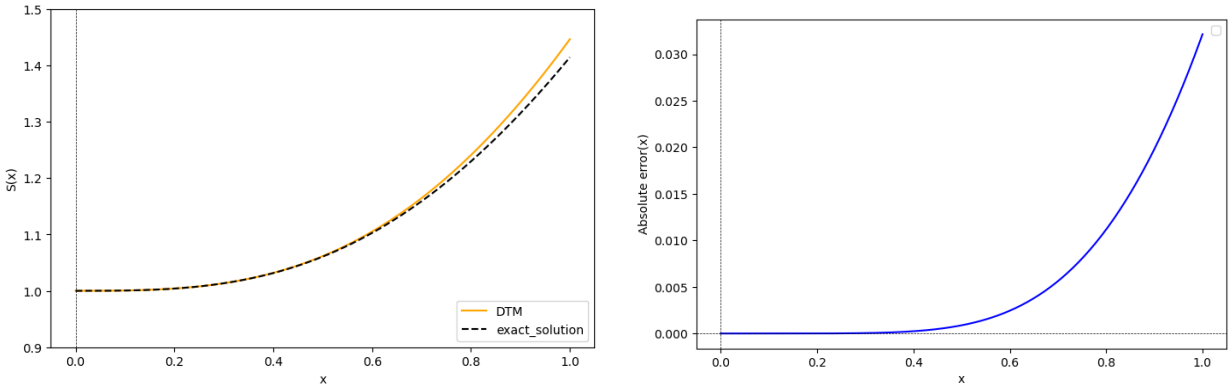


FIGURE 2. Comparison between exact solution and DTM solution of order 9 (left panel) and the related absolute error (right panel) in Test problem 3.2.

TABLE 4. Comparison of the exact solution $s(x) = \sqrt{1+x^3}$ with numerical approximations obtained using NCBS, VIM, and DTM methods in Test problem 3.2.

| $x$ | Exact solution | NCBS | VIM | DTM | Absolute error |
|---|---|---|---|---|---|
| 0.0 | 1.0 | 1.0 | 1.0 | 1.0 | 0.0 |
| 0.1 | 1.0004998750624610 | 1.000499880240 | 1.0004998751 | 1.0004999375088541 | $6.244639 \times 10^{-8}$ |
| 0.2 | 1.0039920318408906 | 1.003992049053 | 1.0039920318 | 1.0039960045333334 | $3.972692 \times 10^{-6}$ |
| 0.3 | 1.0134100848126586 | 1.013410089651 | 1.0134100844 | 1.0134546117765626 | $4.452696 \times 10^{-5}$ |
| 0.4 | 1.0315037566582101 | 1.031503779734 | 1.0315037286 | 1.0317463210666666 | $2.425644 \times 10^{-4}$ |
| 0.5 | 1.0606601717798212 | 1.060660175143 | 1.0606594086 | 1.0615407307942708 | $8.805590 \times 10^{-4}$ |
| 0.6 | 1.1027239001672178 | 1.102723927144 | 1.1027128254 | 1.1051732296000000 | $2.449329 \times 10^{-3}$ |
| 0.7 | 1.1588787684654510 | 1.158878768922 | 1.1587753002 | 1.1645042350619792 | $5.625467 \times 10^{-3}$ |
| 0.8 | 1.2296340919151518 | 1.229634119495 | 1.2289362534 | 1.2408043861333333 | $1.117029 \times 10^{-2}$ |
| 0.9 | 1.3149144458861193 | 1.314914439312 | 1.3112512518 | 1.3347152230796875 | $1.980078 \times 10^{-2}$ |
| 1.0 | 1.4142135623730951 | – | – | 1.4463541666666666 | $3.214060 \times 10^{-2}$ |

TABLE 5. Maximum residual error for Test problem 3.2.

| $N$ | 3 | 6 | 9 | 12 | 15 |
|---|---|---|---|---|---|
| $R_N$ | 2.340445 | 0.903506 | 0.993699 | 0.999236 | 0.997156 |

**Test problem 3.3.** *By assigning the parameters $m = 1$, $n = 2$, and $\lambda = 1$, Eq. (1.1) simplifies to the second type of third-order nonlinear EFSDE:*

$$\varepsilon \frac{d^3 s}{dx^3} + \frac{1}{x}\frac{d^2 s}{dx^2} + s = 3\varepsilon\left(-27\varepsilon\cos(3x) + \sin(3x) - \frac{9\sin(3x)}{x}\right). \tag{3.20}$$

*For boundary conditions, setting $x_0 = 0$, $x_1 = 1$, $s_0 = 0, s_1 = 9\varepsilon$, and $s_2 = 9\varepsilon\sin(3)$, we have Type II boundary conditions:*

$$S(0) = 0, \quad S'(0) = 9\varepsilon, \quad S(1) = 3\varepsilon\sin(3). \tag{3.21}$$

*A straightforward calculation reveals that $s(x) = 3\varepsilon\sin(3x)$ is the true actual solution.*

Rearranging Eq. (3.20) and applying fundamental properties of DTM, the following recursive formula is obtained:

$$\varepsilon\sum_{l=0}^{k}\delta\left(l-1\right)\left(k+3-l\right)\left(k+2-l\right)\left(k+1-l\right)S\left(k+3-l\right)+\sum_{l=0}^{k}\delta(l-1)S(k-l) \tag{3.22}$$

$$+(k+2)(k+1)S(k+2)=3\varepsilon\Bigg(\sum_{l=0}^{k}\delta(l-1)\frac{3^{k-l}}{(k-l)!}\sin\left(\frac{\pi}{2}(k-l)\right)$$

$$-27\varepsilon\sum_{l=0}^{k}\delta(l-1)\frac{3^{k-l}}{(k-l)!}\cos\left(\frac{\pi}{2}(k-l)\right)-9\frac{(3^k)}{k!}\sin\left(\frac{\pi}{2}k\right)\Bigg), \tag{3.23}$$

and the transformed I.C. and B.C. are

$$S(0)=0,\quad S\left(1\right)=9\varepsilon. \tag{3.24}$$

Through the application of DTM, we derive a series-based analytical solution, with coefficients determined computationally via Python. For $k=0$, Eq. (3.22) simplifies to

$$6\varepsilon\delta\left(0-1\right)S(3)+\delta(0-1)S(0)+2S(2)=3\varepsilon\Big(\delta(0-1)\sin\left(0\right)-27\varepsilon\delta(0-1)\cos\left(0\right)-9\sin\left(0\right)\Big). \tag{3.25}$$

Substituting the values from Eq. (3.24) in Eq. (3.25), we get $S(2)=0$. For $k=1$, Eq. (3.22) reduces to

$$\varepsilon\sum_{l=0}^{1}\delta\left(l-1\right)\left(4-l\right)\left(3-l\right)\left(2-l\right)S\left(4-l\right)+\sum_{l=0}^{1}\delta(l-1)S(1-l)+6S(3)$$

$$=3\varepsilon\left(\sum_{l=0}^{1}\delta(l-1)\frac{3^{1-l}}{(1-l)!}\sin\left(\frac{\pi}{2}(1-l)\right)-27\varepsilon\sum_{l=0}^{1}\delta(l-1)\frac{3^{1-l}}{(1-l)!}\cos\left(\frac{\pi}{2}(1-l)\right)-27\sin\left(\frac{\pi}{2}\right)\right). \tag{3.26}$$

Substituting the values from Eq. (3.24) and $S(2)=0$ in Eq. (3.26), we get

$$S(3)=\frac{3\varepsilon\left(-27\varepsilon-27\right)}{6\varepsilon+6}.$$

For $k=2$, Eq. (3.22) reduces to

$$\varepsilon\sum_{l=0}^{2}\delta\left(l-1\right)\left(5-l\right)\left(4-l\right)\left(3-l\right)S(5-l)+\sum_{l=0}^{2}\delta(l-1)S(2-l)+12S(4)$$

$$=3\varepsilon\left(\sum_{l=0}^{2}\delta(l-1)\frac{3^{2-l}}{(2-l)!}\sin\left(\frac{\pi}{2}(2-l)\right)-27\varepsilon\sum_{l=0}^{2}\delta(l-1)\frac{3^{2-l}}{(2-l)!}\cos\left(\frac{\pi}{2}(2-l)\right)-9\frac{(3^2)}{2!}\sin\left(\pi\right)\right). \tag{3.27}$$

Substituting the values from Eq. (3.24), $S(2)$, and $S(3)$ in Eq. (3.27), we get $S(4)=0$. For $k=3$, Eq. (3.22) reduces to

$$\varepsilon\sum_{l=0}^{3}\delta\left(l-1\right)\left(6-l\right)\left(5-l\right)\left(4-l\right)S\left(6-l\right)+\sum_{l=0}^{3}\delta(l-1)S(3-l)+20S(5)$$

$$=3\varepsilon\Bigg(\sum_{l=0}^{3}\delta(l-1)\frac{3^{3-l}}{(3-l)!}\sin\left(\frac{\pi}{2}(3-l)\right)-27\varepsilon\sum_{l=0}^{3}\delta(l-1)\frac{3^{3-l}}{(3-l)!}\cos\left(\frac{\pi}{2}(3-l)\right) \tag{3.28}$$

$$-9\frac{(3^3)}{3!}\sin\left(\frac{3\pi}{2}\right)\Bigg).$$

Substituting the values from Eq. (3.24), $S(2)$, $S(3)$ and $S(4)$ in Eq. (3.28), we get $S(5)=\frac{240\varepsilon}{40}$. Similarly, substituting different values of $k$ in Eq. (3.22) and using evaluated coefficients, we can find the values $S(k)$ for $k\geq 6$. Using the

definition of inverse transform from Eq. (2.2), we get an approximate series solution:

$$s(x) = 9\varepsilon x - \frac{27\varepsilon}{2}x^3 + \frac{243\varepsilon}{40}x^5 + \frac{729\varepsilon}{560}x^7 + \frac{729\varepsilon}{4480}x^9 + \dots. \tag{3.29}$$

Let us consider $\varepsilon = 1$ in Eq. (3.29) to get

$$s(x) = 9x - \frac{27x^3}{2} + \frac{243x^5}{40} - \frac{729x^7}{560} + \frac{729x^9}{4480} + \dots, \tag{3.30}$$

which coincides with the Taylor expansion series form of the true solution $s(x) = 3\varepsilon \sin 3x$. To show the convergence of the approximate series solution obtained by DTM of Test problem 3.3 given in Eq. (3.20) and from Corollary 2.5 we have,

$$\gamma_0 = \frac{\|\zeta_1\|}{\|\zeta_0\|} < 1, \quad \gamma_1 = \frac{\|\zeta_2\|}{\|\zeta_1\|} < 1, \quad \gamma_2 = \frac{\|\zeta_3\|}{\|\zeta_2\|} < 1, \quad \dots.$$

Therefore for the series form Eq. (3.32), one obtains that $\gamma_n$ tends to 0 as $n$ increased. Therefore, from Corollary 2.5 we can say that the obtained approximate solution is convergent to the actual solution. For comparison and visualization

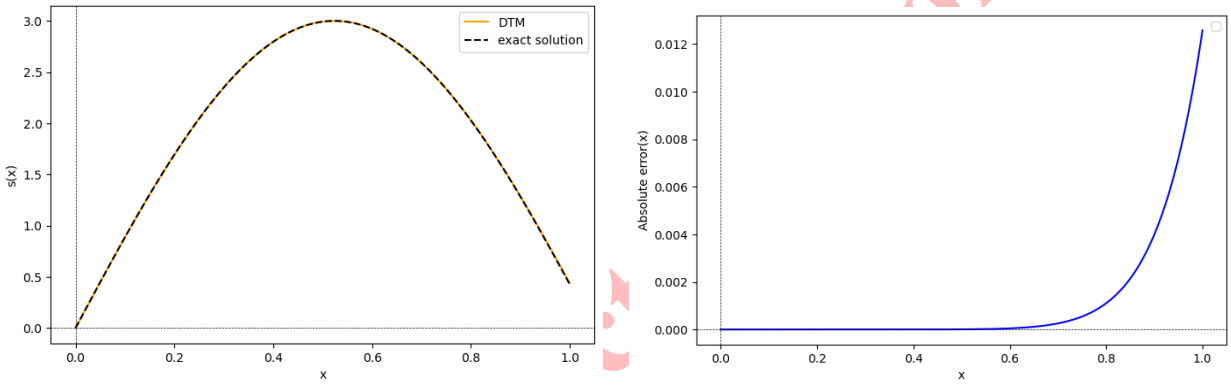


FIGURE 3. Comparison between exact solution and DTM solution of order 9 (left panel) and the related absolute error (right panel) in Test problem 3.2.

TABLE 6. Comparison between the exact solution and the DTM approximation for various values of $x$ in Test problem 3.3.

| $x$ | Exact solution | DTM | Absolute Error |
|---|---|---|---|
| 0.0 | 0.0 | 0.0 | 0 |
| 0.1 | 0.8865606199840188 | 0.8865606199841518 | $1.330047 \times 10^{-13}$ |
| 0.2 | 1.6939274201851064 | 1.6939274204571428 | $2.720364 \times 10^{-10}$ |
| 0.3 | 2.3499807288824500 | 2.3499807523453122 | $2.346286 \times 10^{-8}$ |
| 0.4 | 2.7961172579016793 | 2.7961178112000000 | $5.532983 \times 10^{-7}$ |
| 0.5 | 2.9924849598121632 | 2.9924913678850444 | $6.408073 \times 10^{-6}$ |
| 0.6 | 2.9215428926345860 | 2.9215902065142860 | $4.731388 \times 10^{-5}$ |
| 0.7 | 2.5896280999466220 | 2.5898840673890633 | $2.559674 \times 10^{-4}$ |
| 0.8 | 2.0263895416534520 | 2.0274920886857135 | $1.102547 \times 10^{-3}$ |
| 0.9 | 1.2821396407014893 | 1.2861289856430789 | $3.989345 \times 10^{-3}$ |
| 1.0 | 0.4233600241796016 | 0.4359374999999996 | $1.257748 \times 10^{-2}$ |

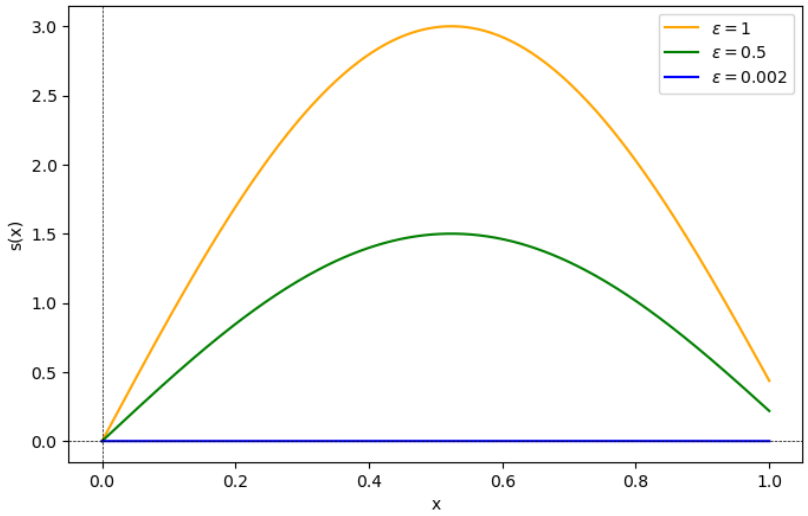


FIGURE 4. Impact of $\varepsilon$ on the $s(x)$.

of the analytic solution generated by DTM of order 9 and the exact solution, we have plotted the graph in Figure 3 for different values of $x$. Figure 3 demonstrates excellent agreement between the approximate series solution obtained by DTM of order 9 and the actual solution for diverse values of $\varepsilon = 1$. The solution obtained by DTM of order 9 is compared with the true actual solution for accuracy assessment in Table 6. From Table 6, it is evident that the DTM gives good agreement with the true solution. The accuracy assessment of DTM, quantified through absolute errors, appears in Table 6. Figure 4 illustrates the numerical solutions for three representative values of $\varepsilon = 1$, $\varepsilon = 0.5$, and $\varepsilon = 0.002$.

The behaviour of the solution $s(x)$ to the third-order differential equation given in Eq. (3.20), subject to the Type II boundary conditions defined in Eq. (3.21), is significantly influenced by the value of parameter $\varepsilon$. As observed, for larger values of $\varepsilon$, such as $\varepsilon = 1$, the solution exhibits pronounced nonlinear behaviour, reaching a higher peak near the midpoint of the domain. As $\varepsilon$ decreases, the amplitude of the solution reduces significantly. In the case of $\varepsilon = 0.002$, the solution remains nearly flat and close to zero throughout the interval, indicating that the influence of the higher-order derivative terms becomes negligible in the limit of small $\varepsilon$. This analysis demonstrates that the solution is highly sensitive to the magnitude of $\varepsilon$, which governs the contribution of the third derivative term. For small $\varepsilon$, the dominant dynamics are driven by the lower-order terms, leading to a flatter solution profile. Conversely, larger $\varepsilon$ values amplify the effects of the higher-order term, resulting in stronger curvature and a more prominent response. To evaluate the performance of the DTM on the second type of third-order nonlinear exponentially fractional singular

TABLE 7. Maximum residual error for Test problem 3.3.

| $N$ | 5 | 7 | 9 | 11 | 13 |
|---|---|---|---|---|---|
| $R_N$ | 19.104301 | 1.408994 | $5.583295 \times 10^{-2}$ | $1.380933 \times 10^{-3}$ | $2.334239 \times 10^{-5}$ |

differential equation (EFSDE) described by Eq. (3.20), the maximal residual error was computed for increasing values of the DTM series order $N$. The problem is subject to Type II boundary conditions defined in Eq. (3.21), with an exact solution given by $s(x) = 3\varepsilon \sin(3x)$. The residual error results are presented in Table 7. It is evident from the results that the maximum residual error decreases significantly with increasing series order. Specifically, the error drops from 19.104301 at $N = 5$ to a remarkably low value of $2.334239 \times 10^{-5}$ at $N = 13$. This trend demonstrates the rapid convergence and high accuracy of the DTM even for strongly nonlinear singular problems. The results confirm that

the DTM not only captures the behavior of the exact solution efficiently but also ensures precision with a relatively low-order approximation. The sharp decline in residual error across increasing $N$ values illustrates the robustness and effectiveness of the method for solving singular boundary value problems involving nonlinear terms.

**Test problem 3.4.** *By assigning the parameters $n = 1, m = 2, \lambda = 1$, Eq. (1.1) simplifies to the second type of third-order nonlinear EFSDE:*

$$\frac{d^3s}{dx^3} + \frac{1}{x}\frac{d^2s}{dx^2} + 4x\left(9 + 22x^4 + x^8\right)e^{-3s} = 0, \quad |x| < 1. \tag{3.31}$$

*For boundary conditions, setting $x_0 = 0, s_0 = s_1 = s_2 = 0$, we have Type I boundary conditions:*

$$s(0) = 0, \quad s'(0) = 0, \quad s''(0) = 0. \tag{3.32}$$

*A straightforward calculation reveals that the exact solution is $s(x) = \ln\left(1 - x^4\right)$.*

Rearranging Eq. (3.31) and applying fundamental properties of DTM, the following recursive formula is obtained:

$$\sum_{l=0}^{k} \delta(l-1)(k+3-l)(k+2-l)(k+1-l)S(k+3-l) + (k+1)(k+2)S(k+2)$$
$$+ \sum_{l=0}^{k}\Big(36\delta(l-2) + 88\delta(l-6) + 4\delta(l-10)\Big)E(k-l) = 0. \tag{3.33}$$

where

$$E(k) = \begin{cases} e^{-3S(0)}, & k = 0, \\ -3\sum\limits_{l=0}^{k-1} \frac{l+1}{k} S(l+1)E(k-l-1), & k \geq 1, \end{cases} \tag{3.34}$$

and the transformed I.C. and B.C. are

$$S(0) = 0, \quad S(1) = 0, \quad S(2) = 0. \tag{3.35}$$

Through the application of DTM, we derive a series-based analytical solution, with coefficients determined computationally via Python. For $k = 1$, Eq. (3.33) simplifies to

$$\sum_{l=0}^{1} \delta(l-1)(4-l)(3-l)(2-l)S(4-l) + 6S(3) + \sum_{l=0}^{1}\Big(36\delta(l-2) + 88\delta(l-6) \tag{3.36}$$
$$+ 4\delta(l-10)\Big)E(1-l) = 0.$$

By placing the values from Eq. (3.35) into Eq. (3.36), we get $S(3) = 0$. For $k = 2$, Eq. (3.36) reduces to

$$\sum_{l=0}^{2} \delta(l-1)(5-l)(4-l)(3-l)S(5-l) + 12S(5) + \sum_{l=0}^{2}\Big(36\delta(l-2) + 88\delta(l-6) \tag{3.37}$$
$$+ 4\delta(l-10)\Big)E(2-l) = 0.$$

Substituting the values from Eq. (3.35) and $S(3) = 0$ in Eq. (3.37), we get $S(4) = -1$. For $k = 3$, Eq. (3.36) reduces to

$$\sum_{l=0}^{3} \delta(l-1)(6-l)(5-l)(4-l)S(6-l) + 20S(5) + \sum_{l=0}^{3}\Big(36\delta(l-2) + 88\delta(l-6) \tag{3.38}$$
$$+ 4\delta(l-10)\Big)E(3-l) = 0.$$

Substituting the values from Eq. (3.35), $S(3)$, and $S(4)$ in Eq. (3.38), we get $S(5) = 0$. Similarly, substituting different values of $k$ in Eq. (3.22) and using evaluated coefficients, we can find the values $S(k)$ for $k \geq 6$. Using the definition of inverse transform from Eq. (2.2), we get an approximate series solution:

$$s(x) = -x^4 - \frac{1}{2}x^8 - \frac{1}{3}x^{12} - \frac{1}{4}x^{16} - \frac{1}{5}x^{20} + \dots. \tag{3.39}$$

The residual error corresponding to various values of $N$ for Eq. (3.31) is presented, revealing a significant reduction as the number of terms increases which is clear from Table 9. Specifically, the maximum residual error drops from $\mathcal{O}(10^0)$ at $N = 8$ to $\mathcal{O}(10^{-3})$ at $N = 20$, highlighting the convergence behaviour of the DTM. This consistent decrease affirms the accuracy and reliability of the differential transform method in approximating the exact solution $s(x) = \ln(1-x^4)$. The results demonstrate that even with moderately small values of $N$, the method achieves a high degree of precision. Such performance supports the applicability of DTM in solving singular, nonlinear EFSDEs with complex exponential forcing terms. To show the convergence of the approximate series solution obtained by DTM of Test problem 3.4

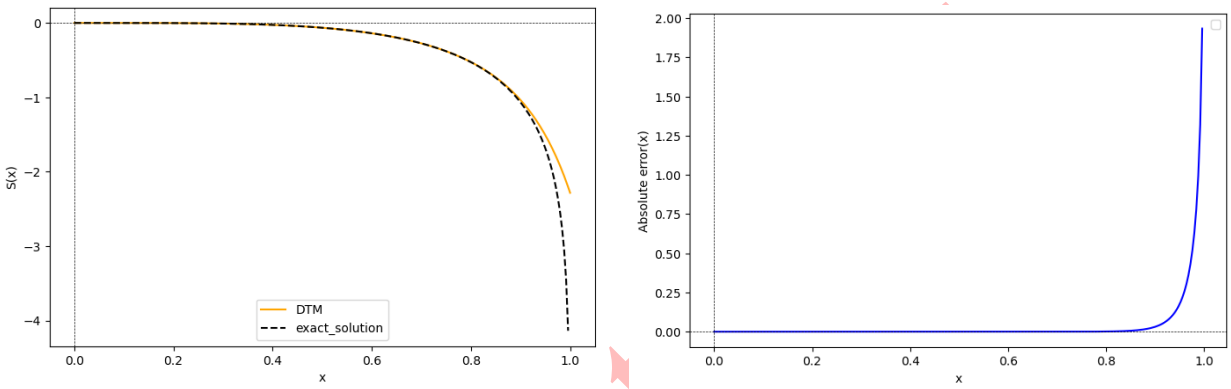


FIGURE 5. Comparison between exact solution and DTM solution of order 9 (left panel) and the related absolute error (right panel) in Test problem 3.4.



TABLE 8. Comparison of the exact solution $s(x) = \ln(1 - x^4)$ and analytical solution in Test problem 3.4.

| $x$ | Exact solution | DTM | Absolute error |
|---|---|---|---|
| 0.0 | 0.0 | 0.0 | 0.0 |
| 0.1 | −0.0001000050003333 | −0.0001000050003334 | $1.103176 \times 10^{-17}$ |
| 0.2 | −0.0016012813669739 | −0.0016012813669738 | $4.835542 \times 10^{-17}$ |
| 0.3 | −0.0081329832301890 | −0.0081329832301416 | $4.739785 \times 10^{-14}$ |
| 0.4 | −0.0259333820265044 | −0.0259333819785390 | $4.796543 \times 10^{-11}$ |
| 0.5 | −0.0645385211375712 | −0.0645385106404623 | $1.049711 \times 10^{-8}$ |
| 0.6 | −0.1388024028804588 | −0.1388015141765665 | $8.887039 \times 10^{-7}$ |
| 0.7 | −0.2745684333063978 | −0.2745281751971685 | $4.025811 \times 10^{-5}$ |
| 0.8 | −0.5269550056958744 | −0.5257352896723135 | $1.219716 \times 10^{-3}$ |
| 0.9 | −1.0674043615439166 | −1.0361176194664101 | $3.128674 \times 10^{-2}$ |

TABLE 9. Maximum residual error for Test problem 3.4.

| $N$ | 8 | 12 | 16 | 20 | 25 |
|---|---|---|---|---|---|
| $R_N$ | $1.060843 \times 10^{0}$ | $1.216803 \times 10^{-1}$ | $1.210531 \times 10^{-2}$ | $1.102876 \times 10^{-3}$ | $2.334239 \times 10^{-5}$ |

given in Eq. (3.31) and from Corollary 2.5 we have,

$$\gamma_0 = \frac{\|\zeta_1\|}{\|\zeta_0\|} < 1, \quad \gamma_1 = \frac{\|\zeta_2\|}{\|\zeta_1\|} < 1, \quad \gamma_2 = \frac{\|\zeta_3\|}{\|\zeta_2\|} < 1, \quad \ldots.$$

Therefore, for the series form Eq. (3.39), we have $\gamma_n \to 0$, as $n \to \infty$. Therefore, from Corollary 2.5 we can say that the obtained approximate solution is convergent to the exact solution.

## 4. CONCLUSION

In this work, the Differential Transform Method (DTM) has been effectively employed to solve third-order nonlinear and singular Emden-Fowler-type differential equations with both Type I and Type II boundary conditions. The method demonstrates excellent agreement with exact solutions, supported by a detailed residual error analysis showing rapid convergence and high accuracy with minimal computational effort. The study highlights DTM's capability to handle strongly nonlinear terms and complex boundary structures without numerical instability. These features underline its potential as a reliable and efficient tool for solving a broad class of nonlinear differential equations in mathematical modeling and applied sciences.

**Data availability:** Data sharing not applicable to this article as no datasets were generated or analyzed during the current study.

**Conflicts of interest:** The authors declare no conflicts of interest.



## REFERENCES


[1] M. Abd El-Hady, H. Emadifar, G. I. El-Baghdady, and A. El-shenawy, *Numerical study of the singular nonlinear initial value problem with applications in astrophysics*, Results Phys., *30* (2025), 108126.

[2] I. H. Abdel-Halim Hassan, *Application to differential transformation method for solving systems of differential equations*, Appl. Math. Model., *32*(12) (2008), 2552–2559.

[3] M. Abdelhakem and Y. H. Youssri, *Two spectral Legendre's derivative algorithms for Lane-Emden, Bratu equations, and singular perturbed problems*, Appl. Numer. Math., *169* (2021), 243–255.

[4] W. M. Abd-Elhameed, Y. Youssri, and E. H. Doha, *New solutions for singular Lane-Emden equations arising in astrophysics based on shifted ultraspherical operational matrices of derivatives*, Comput. Methods Differ. Equ., *2*(3) (2014), 171–185.

[5] H. M. Ahmed, *Numerical solutions for singular Lane-Emden equations using shifted Chebyshev polynomials of the first kind*, Contemp. Math., *4*(1) (2023), 132–149.

[6] M. P. Alam and A. Khan, *An efficient collocation algorithm for third order non-linear Emden–Fowler equation*, Soft Comput., *29* (2025), 1767–1788.

[7] K. Aruna and A. R. Kanth, *A novel approach for a class of higher order nonlinear singular boundary value problems*, Int. J. Pure Appl. Math., *84*(4) (2013), 321–329.

[8] S. Chandrasekhar, *An Introduction to the Study of Stellar Structure*, Dover Publications, New York, NY, USA, 1967.

[9] H. T. Davis, *Introduction to Nonlinear Differential and Integral Equations*, Dover, New York, 1962.

[10] E. H. Doha, W. M. Abd-Elhameed, and Y. H. Youssri, *Second kind Chebyshev operational matrix algorithm for solving differential equations of Lane–Emden type*, New Astron., *23* (2013), 113–117.

[11] U. Flesch, *The distribution of heat sources in the human head: a theoretical consideration*, J. Theor. Biol., *54*(2) (1975), 285–287.

[12] Y. Q. Hasan and L. M. Zhu, *Solving singular boundary value problems of higher-order ordinary differential equations by modified Adomian decomposition method*, Commun. Nonlinear Sci. Numer. Simul., *14*(6) (2009), 2592–2596.
[13] M. K. Iqbal, M. Abbas, and I. Wasim, *New cubic B-spline approximation for solving third order Emden–Flower type equations*, Appl. Math. Comput., *331* (2018), 319–33.
[14] M. Izadi and P. Roul, *A highly accurate and computationally efficient technique for solving the electrohydrodynamic flow in a circular cylindrical conduit*, Appl. Numer. Math., *181* (2022), 110–124.
[15] M. Izadi and P. Roul, *A new approach based on shifted Vieta-Fibonacci-quasilinearization technique and its convergence analysis for nonlinear third-order Emden-Fowler equation with multi-singularity*, Commun. Nonlinear Sci. Numer. Simul., *117* (2023), 106912.
[16] M. Izadi and H. M. Srivastava, *The reaction-diffusion models in biomedicine: highly accurate calculations via a hybrid matrix collocation algorithm*, Appl. Sci., *13*(21) (2023), 11672.
[17] M. Izadi, K. J. Ansari, and H. M. Srivastava, *A highly accurate and efficient Genocchi-based spectral technique applied to singular fractional-order boundary-value problems*, Math. Methods Appl. Sci., *48*(1) (2025), 905–925.
[18] M. Izadi and A. Atangana, *Computational analysis of a class of singular nonlinear fractional multi-order heat conduction model of the human head*, Sci. Rep., *14* (2024), 3466.
[19] M. Izadi, Ş. Yüzbaşı, and D. Kumar, *A hybrid numerical approach to solve multi-singular and nonlinear Emden–Fowler equations of fourth order: HQLMT*, Iran. J. Sci., *48*(4) (2024), 917–930.
[20] A. Khan, M. Faheem, and A. Raza, *Solution of third-order Emden-Fowler-type equations using wavelet methods*, Eng. Comput., *38*(6) (2021), 2850–2881.
[21] M. Lakestani and B. N. Saray, *Numerical solution of singular IVPs of Emden-Fowler type using Legendre scaling functions*, Int. J. Nonlinear Sci., *13*(2) (2012), 211–219.
[22] H. J. Lane, *On the law of electrical conduction in metals*, Am. J. Phys., *i* (1846), 230–241.
[23] S. Lin, *Oxygen diffusion in a spherical cell with nonlinear oxygen uptake kinetics*, J. Theoret. Biol., *60*(2) (1976), 449–457.
[24] S. Mckee, R. Watson, J. A. Cuminato, J. Caldwell, and M. S. Chen, *Calculation of electro-hydrodynamic flow in a circular cylindrical conduit*, Z. Angew. Math. Mech., *77* (1977), 457–465.
[25] Y. F. Patel and J. M. Dhodiya, *Efficient algorithm to study the class of Burger's Fisher equation*, Int. J. Appl. Nonlinear Sci., *3*(3) (2022), 242–266.
[26] Y. F. Patel and J. M. Dhodiya, *A semi-analytic approach to study propagation and amplification of tsunami waves in mid-ocean and their run-up on shore*, Nonlinear Dyn., *111*(15) (2023), 14409–14419.
[27] Y. F. Patel and M. Izadi, *An analytical investigation of nonlinear time-fractional Schrödinger and coupled Schrödinger-KdV equations*, Result Phys., *70* (2025), 108137.
[28] N. Patel and R. Meher, *Analytical investigation of Jeffery-Hemal flow with magnetic field by differential transform method*, Int. J. Adv. Appl. Math. Mech., *6* (2018), 1–9.
[29] R. Picanco, M. Malheiro, and S. Ray, *Charged polytropic stars and a generalization of Lane-Emden equation*, Int. J. Modern Phys. D, *13*(07) (2004), 1441–1445.
[30] R. Rach, J. S. Duan, and A. M. Wazwaz, *On the solution of non-isothermal reaction-diffusion model equations in a spherical catalyst by the modified Adomian method*, Chem. Eng. Commun., *202*(8) (2015), 1081–1088.
[31] H. Ramos and M. A. Rufai, *An adaptive pair of one-step hybrid block Nyström methods for singular initial-value problems of Lane-Emden-Fowler type*, Math. Comput. Simul., *193* (2022), 497–508.
[32] J. L. Ramos, *Linearization methods in classical and quantum mechanics*, Comput. Phys. Commun., *153*(2) (2003), 199–208.
[33] Z. Sabir, M. A. Z. Raja, D. Baleanu, K. Cengiz, and M. Shoaib, *Design of Gudermannian neuroswarming to solve the singular Emden-Fowler nonlinear model numerically*, Nonlinear Dyn., *106*(4) (2021), 3199–3214.
[34] J. Shahni, R. Singh, and C. Cattani, *Bernoulli collocation method for the third-order Lane-Emden-Fowler boundary value problem*, Appl. Numer. Math., *186* (2023), 100–113.
[35] R. Singh and M. Singh, *An optimal decomposition method for analytical and numerical solution of third-order Emden-Fowler type equations*, J. Comput. Sci., *63* (2022), 101790.

[36] H. R. Swathi and T. C. Sushma, *DTM approach on certain differential equations in real life applications*, Int. J. Math. Trends Techn., *69*(2) (2023), 91–97.
[37] K. Swati, A. K. Singh and M. Verma, *Higher order Emden-Fowler type equations via uniform Haar Wavelet resolution technique*, J. Comput. Appl. Math., *376* (2020), 112836.
[38] A. Verma and M. Kumar, *Numerical solution of third-order Emden-Fowler type equations using artificial neural network technique*, Euro. Phys. J. Plus, *135* (2020), 751.
[39] A. M. Wazwaz, *Solving two Emden-Fowler type equations of third order by the variational iteration method*, Appl. Math. Inform. Sci., *9*(5) (2011), 2429.
[40] A. M. Wazwaz, R. Rach, L. Bougoffa, and J. S. Duan, *Solving the Lane-Emden-Fowler type equations of higher orders by the Adomian decomposition method*, Comput. Model. Eng. Sci., *100*(6) (2014), 507–529.
[41] Y. H. Youssri and A. G. Atta, *Spectral collocation approach via normalized shifted Jacobi polynomials for the nonlinear Lane-Emden equation with fractal-fractional derivative*, Fractal Fract., *7*(2) (2023), 133.
[42] F. Zabihi, *The use of the Sinc-collocation method for solving steady-state concentrations of carbon dioxide absorbed into phenyl glycidyl ether*, Comput. Methods Differ. Equ., *12*(4) (2024), 857–865.